Preparation, Characterization, and Gas Permeation Properties of Carbon Molecular Sieve Membranes Derived from Dense P84-Polyimide Film

Ho Bum Park, Sang Yong Nam*, Jeong Gyu Jang, and Young Moo Lee[†]

National Research Laboratory for Membrane, School of Chemical Engineering, College of Engineering,
Hanyang University, Seoul 133-791, Korea
*Department of Polymer Science and Engineering, College of Engineering, Gyeongsang National University, Chinju 660-701, Korea

Abstract : The gas permeation properties have been studied on carbon molecular sieve (CMS) membranes prepared by pyrolysis of P84 polyimide under various conditions. P84 polyimide shows high permselectivities (O_2/N_2 = 9.17 and CO_2/N_2 = 35) for various gas pairs and has a good processibility because it is easily soluble in high polar solvents such as N-methylpyrrolidinone (NMP), dimethylformamide (DMF), and N,N-dimethylacetamide (DMAc). After pyrolysis under Ar flow, the change in the heating rate was found to affect the gas permeation properties to some extent. The permeabilities of the selected gases were shown to be in the order He > CO_2 > O_2 > N_2 for all the CMS membranes, whose order was in accordance with the order of kinetic gas diameters. It also revealed that the pyrolysis temperature considerably influenced the gas permeation properties of the CMS membranes derived from P84 polyimide. The CMS membranes pyrolized at 700℃ temperature exhibited the highest permeability with relatively large loss in permselectivity. This means that the pyrolysis temperature should be varied in accordance with target gases to be separated.

Keywords : carbon molecular sieve membrane; gas separation; pyrolysis; P84 polyimide

1. Introduction

Carbon is one of the most common materials used in day by day human activity, and is found interests in materials having a wide range of properties: charcoal, battery electrodes, and composite. Particularly, microporous carbon materials exist as a powder, as granules, or in a fibrous form, and microporous carbon is anticipated to be useful as an adsorbent for the pressure swing adsorption (PSA) process and as a shape-selective catalyst support.

In the field of membrane-based gas separation, carbon molecular sieve (CMS) films have been extensively investigated owing to their excellent permselectivity and permeability. At present, CMS membranes are typically produced from pyrolysis of a polymeric precursor, such as poly(furfuryl alcohol) [1], poly(vinylidene chloride) [2], phenolic resin [3], polyimides [4-10], and poly(imide siloxane) [11-13]. In particular, polyimide films as thermoresistant polymers were found to give a graphite film with rather high crystallinity through a simple heat treatment under atmospheric pressure. Because of the practical and promising applications of polyimide films, there have
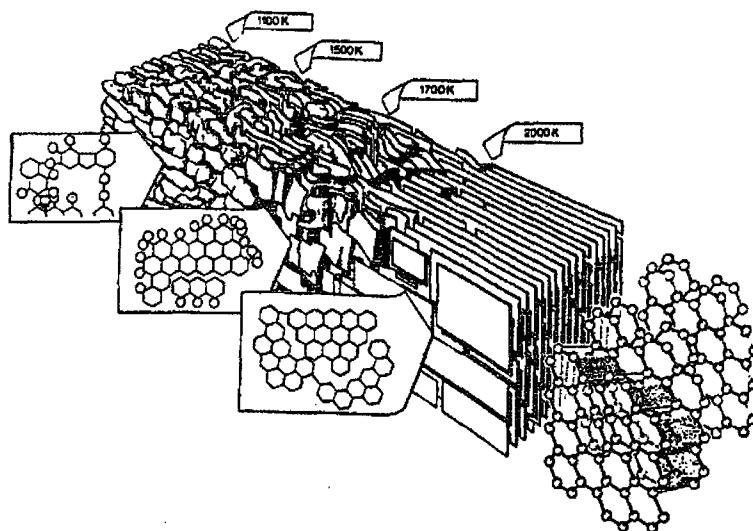
[†]주저자(e-mail : ymlee@hanyang.ac.kr)

Fig. 1. Structural formation of carbon membranes derived from organic polymeric precursors at various temperatures.

been commercially available films with different molecular structures, giving a wide variety of structure in the carbon molecular sieve membranes after heat treatment at high temperatures. As shown in Fig. 1 [14], in the case of the carbons prepared by the pyrolysis of organic polymers such as polyimides between 600 and 2200℃, the carbon structure obtained is known to have a turbostratic structure, in which planar layers of graphite-like microcrystals are dispersed in a noncrystalline and amorphous carbon. Indeed, the nanometric texture in the cross-section of carbon films derived from Kapton polyimide by heat treatment changes from turbostratic (650-1000℃) to turbostratic with flattened pores (2200℃), partially graphitic (2300℃), mostly graphitic (2500℃), and finally graphitic (3000℃).

The CMS membranes fabricated from these polymeric precursors are commonly non-crystalline, but they can be partially crystalline, being composed of basic structural units of planar graphitic microcrystallites embedded in sp^3 hybridized carbon clusters. These clusters can be concentric or be randomly oriented within the basic structural units. The formation of bent graphene layers has been observed, and completely amorphous structures with no

Fig. 2. A TEM image of CMS membrane prepared from pyrolysis of P84 polyimide up to 800℃.

detectable basic structural units have been shown to exist. Generally, these CMS membrane materials have disordered building blocks, which consist of aromatic microdomains. Mircovoids in the carbon matrices are formed because of the misalignment of the aromatic microdomains (so-called amorphous carbons), as shown in Fig. 2, which is a TEM image of a CMS membrane produced by pyrolysis at 800℃ of P84

polyimide used as the precursor of CMS membrane in this study. Here, no ordered structural building units were observed only an amorphous carbon structure. These microvoids create the ultramicroporosity of the carbon matrix and are formed by channeling the molecular debris through a thermosetting polymer matrix during controlled pyrolysis or by carbonization of synthetic and natural hydrocarbon precursors.

In the preparation of CMS membranes, the factors determining the gas permeation properties and microstructures of CMS membranes are significantly affected by several factors and kinds of polymeric precursors. These factors can be addressed as follows: (a) the pyrolysis conditions, (b) the choice of polymeric precursors, and (c) the type of membrane geometry.

The pyrolysis conditions such as the heating rate and the pyrolysis temperature are important factors in the preparation of optimized CMS membranes. Many researchers have investigated on the effect of the pyrolysis conditions on the microstructures and gas permeation properties of the CMS membranes [15-18]. Usually, all the pyrolysis temperatures used in the literatures fall within the range 500-1000°C. The heating rate, typically 1-10°C/min, can also affect the CMS membrane performance.

Many studies have shown that numerous polymeric precursors possess properties which make them suitable as precursors for CMS membranes [19-21]. In addition, CMS membranes from many polymeric precursors present different membrane configurations: asymmetric capillary membranes, symmetric flat membranes, supported asymmetric membranes, and supported tubular membranes.

From a practical point of view, the high cost of polyimides is a key factor that limits severely their utilization in the preparation of CMS membranes. In this paper, the selection of commercially available P84 polyimide instead of polyimides prepared at the laboratory scale will contribute to the development of CMS membranes. That is, the present work describes

a simple method for preparing CMS membranes from inexpensive polyimides in a single casting step. The properties of resulting CMS membranes for the separation of permanent gases (He/N_2, O_2/N_2, and CO_2/N_2) are also reported.

2. Experimental

2.1. Polymeric Precursor-P84 Polyimide

A commercially-available P84 polyimide (Lenzing P84 polyimide, HP Polymer Inc. of Lewisville, TX, U.S.A.) was chosen as a polymeric precursor for the preparation of carbon membranes. P84 polyimide used in this study is a copolymer with the structure shown in Fig. 3. This material can be prepared by polycondensation of an anhydride (benzophenonetetrac-arboxylic acid dianhydride, BTDA) with aromatic diisocyanates (methylene diphenyl diisocyanate, MDI, and 2, 4-toluene diisocyanate, TDI) in high polar solvents like dimethylformamide (DMF) or dimethyl-acetamide (DMAC).

The thermal properties of the fully amorphous P84-polyimide are characterized by the glass transition temperature of 315°C. The density of P84 polyimide is about 1.41 g/cm^3. The molecular structure in P84 polyimide is likely to be highly disordered. Therefore, this material is expected to be non-graphitizable after pyrolysis at high temperature and results in a significant amount of microporosity.

2.2. Pyrolysis Process and Preparation of CMS Membranes

P84 polyimide films were prepared by drying at 160°C in a vacuum oven for 1 day after solution-casting onto a glass plate. Before each pyrolysis trial, the free-standing P84 polyimide films were rinsed with deionized water and stored at 120°C under a vacuum oven until any residual solvent and dust was completely eliminated. After these pretreatments, the P84 polyimide films were then pyrolyzed in a muffle furnace equipped with an automatic

(a) BTDA   (b) TDI
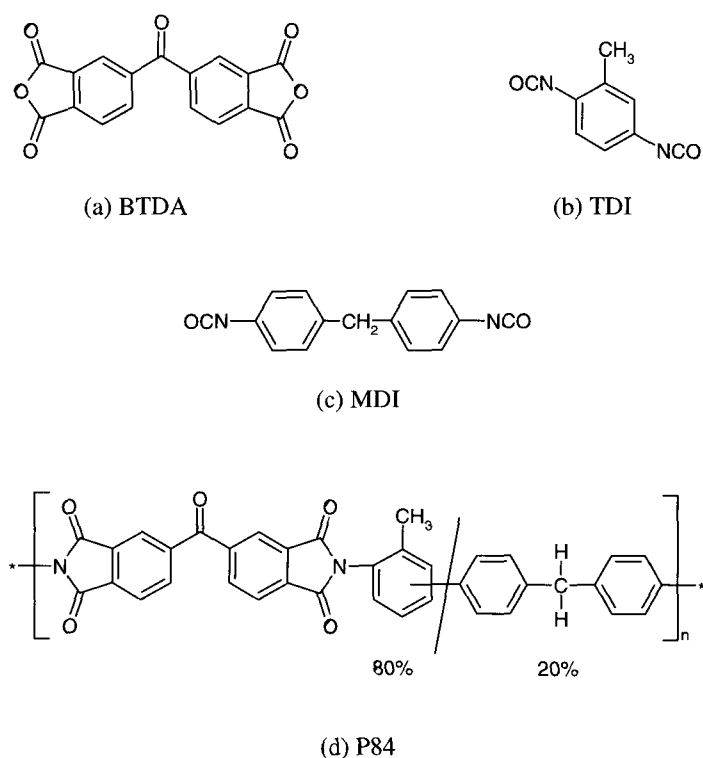
(c) MDI

(d) P84

Fig. 3. Monomers used in the synthesis of P84 polyimide and the basic structure of P84 polyimide.
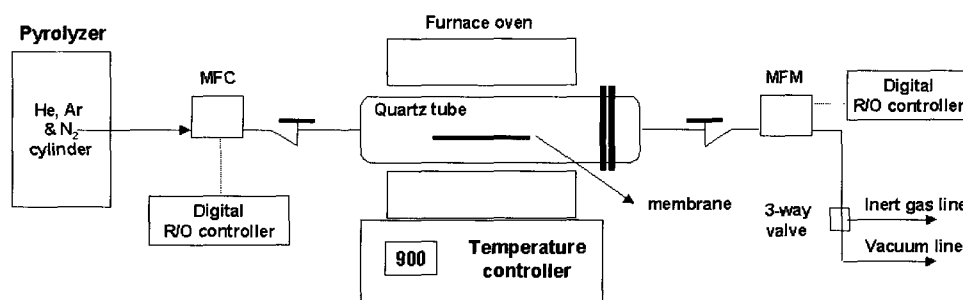

Fig. 4. Schematic diagram of furnace system used in this study.

temperature controller (Laptop, London, U.K.) as shown in Fig. 4.

The CMS membranes were prepared by pyrolysis of P84 polyimide film between alumina plates at mainly 600-800℃ for 3h with a heating rate of 1℃/min and 10℃/min respectively. Pyrolysis atmosphere (Ar flow) was also controlled so as to investigate the effects of pyrolysis conditions on the CMS membrane properties. All the membranes were allowed to cool to room temperature under each atmosphere.

2.3. Characterization Methods

The CMS membranes fabricated from pyrolysis of P84 polyimide films were characterized by the following analysis methods.

(1) Fourier transform infrared (FT-IR) spectroscopy. The ATR-FTIR spectra of P84 polyimide and the CMS membranes were measured by a Nicolet Magna IR 860 instrument (Thermo Nicolet, Madison, WI, U.S.A.) in the range of 4000-500 cm^{-1}.

(2) Thermal gravimetric analysis (TGA). TGA was

carried out in flowing Ar by use of TGA 2050 thermogravimetric analyzer (TA Instruments, New Castle, DE, U.S.A.).

(3) Wide-angle X-ray diffraction (WAXD). An X-ray diffractometer (Rigaku Denki model RAD-C, Rigaku, Tokyo, Japan) was used to evaluate the d spacing of the CMS membranes after pyrolysis.

(4) Elemental analysis (EA). An EA 1110 automatic elemental analyzer (CE Elantech, Inc., Lakewood, NJ, U.S.A.) was used compare the atomic contents (C%, H%, O%, N%) of the CMS membranes before and after pyrolysis.

2.4. Gas Permeation Measurement

The gas permeation properties of P84 polyimide sample and the CMS membranes were also investigated in this study. A constant volume, variable pressure method was used to determine the steady-state pure penetrants permeabilities at 30℃ over a range of upstream pressures up to 76 cmHg. A membrane was loaded into the permeation cell, and degassed by exposing both sides of the membrane to vacuum. After degassing, the upstream side of the membrane was exposed to a fixed pressure of penetrant. The steady-state rate of pressure rise on the downstream side was used to determine the permeability coefficient. At all times during the experiment, the downstream pressure was kept below 1 cmHg. At the steady state, when the rate of downstream pressure rise was constant, the following expression was used to determine the permeability coefficient, P:

$$P = \frac{22,414 \, Vl}{RTAp_{up}} \cdot \frac{dp_{down}}{dt} \qquad (1)$$

where V is the downstream reservoir volume, R is the universal gas constant, T is the absolute temperature, A is the cross-sectional area of the membrane, l is the thickness of membrane, p_{up} is the upstream pressure, and dp_{down}/dt is the rate of change in the downstream
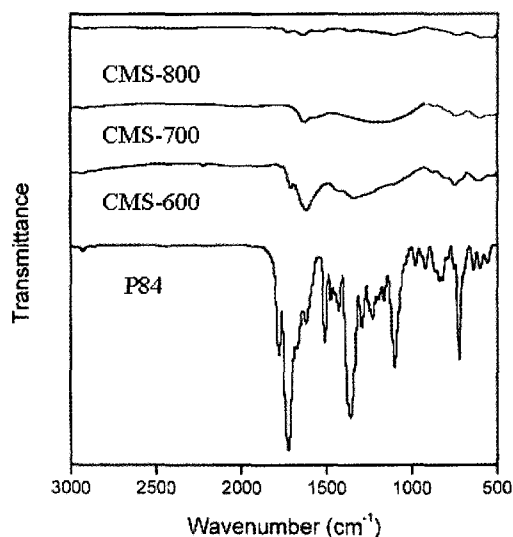

Fig. 5. ATR infrared spectra of P84 polyimide film and CMS membranes pyrolyzed at 600, 700, and 800℃.

pressure. The diffusion coefficient, D, is obtained from the time-lag, θ, as

$$D = \frac{l^2}{6\theta} \qquad (2)$$

3. Results and Discussion

3.1. Characterization

The ATR infrared spectra shown in Fig. 5 indicate that the peak intensities for the aliphatic or aromatic C-N (1100-1200 cm⁻¹, 1300-1400 cm⁻¹), C=O (~1700 cm⁻¹, 1200-1300 cm⁻¹), and C-H bonds (600-900 cm⁻¹, 1000-1200 cm⁻¹) were reduced at higher pyrolysis temperatures.

Table 1 summarizes the elemental contents of the CMS membranes which were heat-treated at the rate of 1℃/min under Ar atmosphere. Hydrogen and oxygen were eliminated more considerably by pyrolysis at higher temperatures, but nitrogen which was contained in imide bonds was rather stable. Generally, the carbonization of the rigid polyimide proceeds in two steps, the first step in the rather narrow temperature range of 550-650℃, showing an

Table 1. Elemental Analysis of CMS Membranes Derived from P84 Polyimide

Heating rate (℃/min)	Pyrolysis temperature(℃)	C(%)	O(%)	N(%)	H(%)
	600	74.1	16.6	6.0	3.2
1	700	86.2	5.6	5.1	3.1
	800	88.7	4.8	4.5	2.0

Table 2. d Spacing of CMS Membranes Calculated from X-ray Diffraction Data

Heating rate (℃/min)	Pyrolysis temperature	d spacing (Å)
	600	4.3
1	700	4.2
	800	3.5
	600	4.5
10	700	4.1
	800	3.7

abrupt weight decrease associated with the evolution of a large amount of carbon monoxide and pronounced shrinkage along the film, and the second step with small weight loss, evolution of small amounts of methane, hydrogen and nitrogen, and little shrinkage over a temperature range from 700℃ to more than 1000℃.

These CMS membranes were essentially X-ray amorphous, and the crystallinity became higher with increasing the pyrolysis temperature. The carbon fabricated by the pyrolysis of organic polymers is known to have a turbostratic structure, in which layer-planes of graphite-like microcrystals are dispersed in a noncrystalline carbon. X-ray diffraction is a useful tool for studying the organization of carbon on a molecular level. Although the interatomic distance (1.41 Å) of same-plane carbon atoms cannot be determined by X-ray diffraction, the d spacing, a reflection of the interplanar distance, can be measured. By analyzing the X-ray diffraction data, the interlayer spacing can be calculated by applying Bragg's equation to the (100) peak as follows

$$d = \frac{\lambda}{2\sin\theta} \tag{3}$$

where d is the d spacing or interlayer distance. Depending on the extent of carbonization and atomic organization, the d spacing for a polymer char can

vary from 5 to 3.354 Å. The average interlayer distance for a perfect graphite crystal is 3.354 Å. Given the morphology of glassy carbon from a polymer precursor, the d spacing cannot be taken as a true measurement of the interlayer distance, but changes in the d spacing can serve as an indicator of the amount of room available for penetrating small molecules.

As shown in Table 2, the d spacing of the CMS membranes derived from P84 polyimide decreased with increasing pyrolysis temperature, irrespective of the heating rate. This means that the average interlayer distance of the CMS membranes decreases with heat treatment, which may be expected to result in high permselectivities for various gas pairs.

TGA curve of P84 polyimide under Ar flow indicates two reaction states (see Fig. 6), which is reflected as two peaks in the differential thermogravimetric (DTG) curve. At the heating rate of 1 Å/ min, P84 polyimide was stable up to approximately 400℃ and lost about 55% of its weight at 1000℃ P84 polyimide started to lose weight at around 200℃, and the weight of P84 polyimide was drastically decreased at 400℃. However, at the heating rate of 10℃/min, the thermal degradation curve was somewhat different when P84 polyimide was thermally decomposed at the heating rate of 1℃/min. That is, the main stages of weight loss shifted up to higher temperature, and also the residual weight at 1000℃
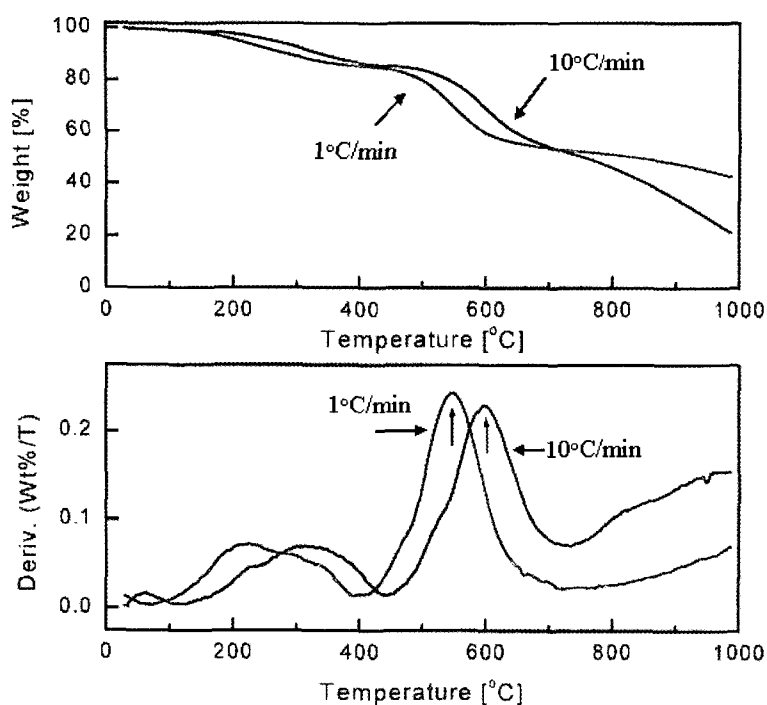
Fig. 6. Thermal gravimetric analysis (TGA) and differential TGA curves of P84 polyimide films.

Table 3. Permeability Data of P-84 Polyimide at 30℃

Permeability (Barrer*)			Selectivity	
P(CO₂)	P(O₂)	P(N₂)	P(CO₂)/P(N₂)	P(O₂)/P(N₂)
0.84	0.22	0.024	35	9.17

* 1 Barrer = $10^{-10} \times cm^3$ (STP) cm/cm²·sec·cmHg

was smaller than the residual weight at the heating rate of 1℃/min. These differences led to the changes in the gas permeation properties of CMS membranes, which will be discussed in the following section.

3.2. Gas Permeation Properties

To evaluate the molecular sieving capability of the CMS membranes derived from P84 polyimide film, single gas permeation experiment was carried out to measure pure component gas permeabilities through the membranes using nitrogen (N₂, 3.64 Å), oxygen (O₂, 3.46 Å), helium (He, 2.60 Å), and carbon dioxide (CO₂, 3.36 Å).

One of the main objectives of this work was to study the effect of pyrolysis conditions on the gas

permeation properties of CMS membranes derived from P84 polyimide. The pyrolysis conditions, including the pyrolysis temperature and the heating rate, are significant factors in determining the microstructure and gas permeation properties of CMS membranes.

In the present work, it was observed that the pyrolysis temperature had a marked influence on the permeation characteristics of the CMS membranes produced. Figs. 7-8 illustrate the He, O₂, N₂, and CO₂ permeabilities at 30℃ for CMS membranes prepared at different pyrolysis temperatures (600, 700, and 800℃). In the case of CMS membranes prepared at the heating rate of 1℃/min, the gas permeabilities reached a maximum at 700℃ for all molecular probes
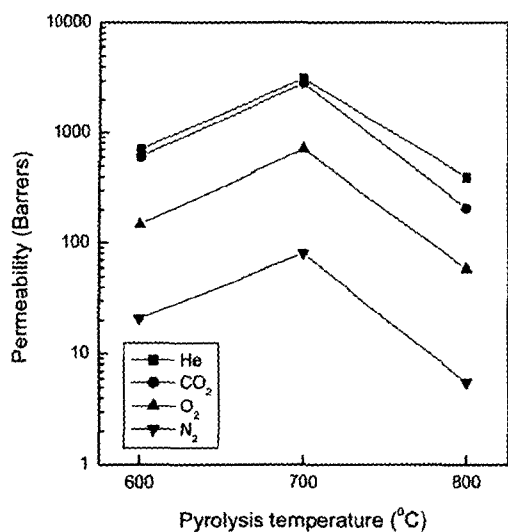
Fig. 7. Gas permeabilities as a function of pyrolysis temperature (heating rate: 1℃/min) for CMS membranes.

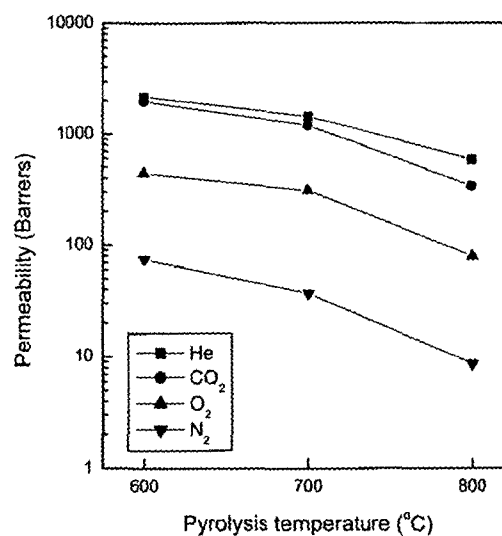Fig. 8. Gas permeabilities as a function of pyrolysis temperature (heating rate: 10℃/min) for CMS membranes.

used. This means that the volume of micropores, based on the mass of the initial polyimide, reached a maximum at 700℃, which might lead to high permeabilities to all gases. In the case of CMS membranes prepared at the heating rate of 10℃/min, however, the pyrolysis temperature decreased permeabilities to all gases but increased gas selectivities without an increase of gas permeability at around 700℃. This indicates that the heating rate influences appreciably the formation process of carbon

membrane, as can be seen in TGA results. Tables 4 and 5 summarizes the gas permeation properties of CMS membranes pyrolyzed at the heating rate of 1℃/min and 10℃/min.
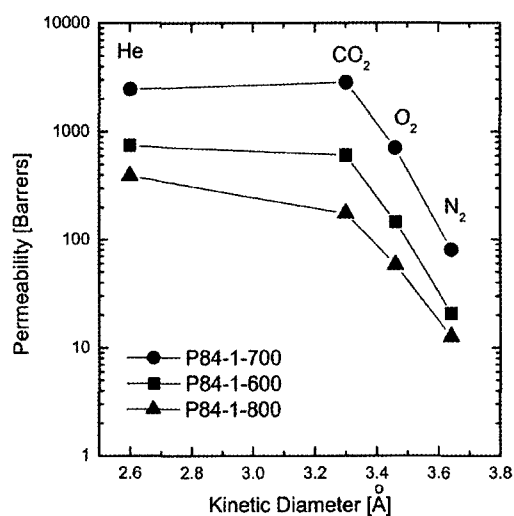
Except CMS membranes prepared at 700℃, the gas permeability decreased with decreasing the heating rate from 10 to 1°C/min. The reason for this trend may be that with decreasing the heating rate the pyrolysis proceeds very slowly, which may make the pore smaller. Additionally, the longer total time for

Table 4. Gas Permeation Data of Carbon Membrane Pyrolyzed at 1℃/min of Heating Rate (measuring temperature: 30℃, membrane thickness: 20 μm)

Sample code	Penetrant	Kinetic Diameters σ[Å]	L-J potential ε/k [K]	Permeability [Barrer]	Selectivity to N_2
P84-1-600	He	2.60	10.2	704.3	33.9
	CO_2	3.30	195	604.1	29.0
	O_2	3.46	107	147.2	7.1
	N_2	3.64	71.4	20.8	-
P84-1-700	He			3162.7	39.3
	CO_2			2854.3	35.5
	O_2			706.4	8.8
	N_2			80.4	-
P84-1-800	He			391.4	71.2
	CO_2			206.3	37.5
	O_2			58.0	10.5
	N_2			5.5	-

Table 5. Gas Permeation Data of Carbon Membrane Pyrolyzed at 10℃/min of Heating Rate (measuring temperature: 30℃, membrane thickness: 20 μm)

Sample code	Penetrant	Kinetic Diameters σ [Å]	L-J potential ε/k [K]	Permeability [Barrer]	Selectivity to N_2
P84-10-600	He	2.60	10.2	2167.4	29.2
	CO_2	3.30	195	1967.4	26.4
	O_2	3.46	107	442.0	5.9
	N_2	3.64	71.4	74.5	-
P84-10-700	He			1445.2	39.2
	CO_2			1192.0	32.3
	O_2			310.9	8.4
	N_2			36.9	-
P84-10-800	He			589.2	68.5
	CO_2			345.0	40.1
	O_2			78.9	9.2
	N_2			8.6	-

Fig. 9. Kinetic diameter of gas vs. gas permeabilities (measured at 30℃) of the CMS membranes prepared at the heating rate of 1℃/min.

pyrolysis may also contribute to the pore size reduction due to a sintering effect.

The permeabilities of the selected gases measured at 30℃ were shown to be in the order of He > CO_2 > O_2 > N_2 for all the CMS membranes (see Fig. 9). The order was in accordance with the order of kinetic gas diameter, since the kinetic diameter sequence is He < CO_2 < O_2 < N_2. Typically, the permeabilities of small gases through microporous membranes are in agreement with the order of the kinetic diameters of

gases, except in some peculiar cases. That is, the gas transport mechanism through these membranes occurs by a diffusion-dominant mechanism or a size-exclusive mechanism.

Separation of small gas pairs such as He/N_2, O_2/N_2, and CO_2/N_2 represents the greatest challenge for membranologists since the kinetic diameter of two gases differs by only a few tenths of an angstrom. In particular, to obtain the high permselectivity of O_2/N_2 and CO_2/N_2, the following strategy should be considered. Generally, the gas permeability, P (Barrer: $10^{-10} \times cm^3 \cdot (STP) \cdot cm/cm^2 \cdot sec \cdot cmHg$) is expressed by the following equation:

$$P_A = D_A \times S_A \qquad (4)$$

The permeability (P_A) of component A can be expressed as the product of a kinetic factor, the diffusion coefficient (D_A), and a thermodynamic factor, the sorption coefficient (S_A). The selectivity A/B is defined as the ratio of the permeabilities P_A and P_B:

D_A/D_B is the ratio of the diffusion coefficients of the two gases and is referred to as the diffusivity selectivity, reflecting the different molecular sizes of gases. S_A/S_B is the ratio of the solubility coefficients of the gases and can be viewed as the solubility

Typical target gas pairs:	O_2/N_2	CO_2/N_2
Range of gas selectivity:	5-20	40-100
Main contribution:	$\alpha_{A/B} = \dfrac{P_A}{P_B} = \left(\dfrac{D_A}{D_B}\right) \cdot \left(\dfrac{S_A}{S_B} \leq 2\right)$	$\alpha_{A/B} = \dfrac{P_A}{P_B} = \left(\dfrac{D_A}{D_B} \leq 4\right) \cdot \left(\dfrac{S_A}{S_B}\right)$
	Diffusion selectivity	Sorption selectivity

Table 6. O_2 and N_2 Diffusion Coefficients $(cm^2 \cdot s^{-1} \times 10^9)$ and Diffusion Selectivity of CMS Membranes Derived from P84 Polyimide

Heating rate		600℃	700℃	800℃
	O_2	4.65	9.17	2.17
1℃/min	N_2	0.60	0.91	0.19
	$D(O_2)/D(N_2)$	7.80	10.10	11.4
	O_2	5.65	10.38	4.51
10℃/min	N_2	0.80	1.10	0.40
	$D(O_2)/D(N_2)$	7.10	9.44	11.28

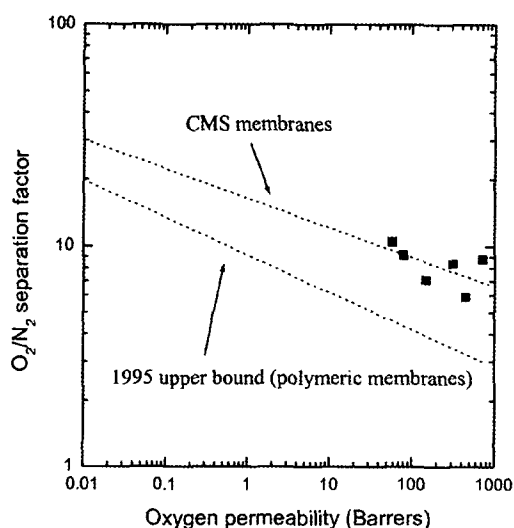**Fig. 10.** O_2 permeability vs. O_2/N_2 selectivity of CMS membranes prepared in this study with upper bound.

(sorption) selectivity, reflecting the relative condensabilities of the gas molecules that interact with polymeric matrices. Commonly, the sorption selectivity terms for O_2/N_2 pair lie in the range of 1-2 for almost all glassy polymers and in the range of 0.7-2 for molecular sieving materials. Therefore, diffusivity selectivity is a significant factor to obtain high permselectivity of membrane material for small gas separation.

The diffusion coefficients and diffusional selectivities of O_2 and N_2 are summarized in Table 6. The diffusional selectivities of CMS membranes derived from P84 polyimide membranes are usually higher than those of typical polymeric membranes. That is, this diffusion-selectivity contribution makes it possible to improve the gas permeability without a large reduction of gas selectivity.

4. Conclusions

The present study shows that carbon molecular sieve (CMS) membranes can be prepared successfully from commercially available polyimide-type polymers. Complex preparation routes such as thermal-imidization of poly(amic acid)-form can be avoided.

The CMS membranes described here possess properties which render them suitable for gas separations of industrial interest, such as O_2/N_2, CO_2/N_2 and He/N_2. Clear differences were found between the separation factors and gas permeation rates obtained from pure gases for P84 polyimide-based CMS membrane. Thus, the characterization of CMS membranes by single gas components underestimates the true separation factor. In addition, gas permeation and separation performance is highly

dependent upon heat treatment conditions (i.e. temperature and heating rate).

Eventually, P84 polyimide is a good candidate material for CMS membrane, and generally CMS membranes derived from P84 polyimide showed very high gas permeabilities without a large loss of selectivity.

Acknowledgements

References

1. M. G. Sedigh, W. J. Onstot, L. Xu, W. L. Peng, T. T. Tsotsis, and M. Sahimi, *J. Phys. Chem. A*, **102**, 8580 (1998).

2. Rao, M. B.; Sircar, S.; Golden, C. US Patent no. 5104425, 14 April **1992**.

3. T. A. Centeno and A. B. Fuertes, *J. Membr. Sci.*, **160**, 201 (1994).

4. M. G. Sedigh, L. Xu, T. T. Tsotsis, and M. Sahimi, *Ind. Eng. Chem. Res.*, **38**, 3367 (1999).

5. J. Hayashi, M. Yamamoto, K. Kusakabe, and S. Morooka, *Ind. Eng. Chem. Res.*, **36**, 2134 (1997).

6. J. Hayashi, M. Yamamoto, K. Kusakabe, and S. Morooka, *J. Membr. Sci.*, **124**, 243 (1997).

7. J. Petersen, M. Matsuda, and K. Haraya, *J. Membr. Sci.*, **131**, 85 (1997).

8. C. W. Jones and W. J. Koros, *Carbon*, **32**, 1419 (1994).

9. A. B. Fuertes, D. M. Nevskaia, and T. A. Centeno, *Microporous and Mesoporous Mater.*, **33**, 115 (1999).

10. K. Wang, H. Suda, and K. Haraya, *Ind. Eng. Chem. Res.*, **40**, 2942 (2001).

11. H. B. Park, I. Y. Suh, and Y. M. Lee, *Chem. Mater.*, **14**, 3034 (2002).

12. H. B. Park and Y. M. Lee, *Membrane J.*, **12**(2), 107 (2002).

13. H. B. Park and Y. M. Lee, *J. Membr., Sci.* 2002, in press.

14. J. W. Patrick (Ed.), Porosity in Carbons: Characterization and Applications, Edward Arnold, London (1995).

15. H. Suda and K. Haraya, *J. Phy. Chem. B*, **101**, 3988 (1997).

16. C. W. Jones and W. J. Koros, *Carbon*, **32**, 1427 (1994).

17. C. W. Jones and W. J. Koros, *Ind. Eng. Chem. Res.*, **34**, 158 (1995).

18. V. C. Geiszler and W. J. Jones, *Ind. Eng. Chem. Res.*, **35**, 2999 (1996).

19. H. C. Foley, *Microporous Mater.*, **4**, 407 (1995).

20. W. Shusen, Z. Meiyun, and W. Zhizhong, *J. Membr. Sci.*, **109**, 267 (1996).

21. A. B. Fuertes and T. A. Centeno, *Microporous and Mesoporous Mater.*, **26**, 23 (1998).